Eur. Phys. J. D **24**, 265–268 (2003)
DOI: 10.1140/epjd/e2003-00159-8

THE EUROPEAN PHYSICAL JOURNAL D

Thermal and chemical nanofractal relaxation

C. Bréchignac[1,a], Ph. Cahuzac[1], F. Carlier[1], C. Colliex[2], M. de Frutos[2], N. Kébaïli[1], J. Le Roux[1], A. Masson[1], and B. Yoon[1]

[1] Laboratoire Aimé Cotton, CNRS, bâtiment 505, Université Paris-Sud, 91405 Orsay Cedex, France
[2] Laboratoire de Physique des solides, bâtiment 510, Université Paris-Sud, 91405 Orsay Cedex, France

Received 10 September 2002
Published online 3 July 2003 –

Abstract. We studied shape relaxation of nano-fractal islands, during annealing, after their growth from antimony cluster deposition on graphite surface. Annealing at 180 °C shows evidence of an increase of the fractal branch width with time followed by branch fragmentation, without changing the fractal dimension. The time evolution of the width of the arm suggests the surface self-diffusion mechanism as the main relaxation process. With Monte Carlo simulations, we confirmed the observed behavior. Comparison is done with our previous results on fragmentation of nano-fractal silver islands when impurity added to the incident cluster promotes rapid fragmentation by surface self-diffusion enhancement [1].

PACS. 61.46.+w Nanoscale materials: clusters, nanoparticles, nanotubes, and nanocrystals – 61.43.Hv Fractals; macroscopic aggregates (including diffusion-limited aggregates) – 81.07.-b Nanoscale materials and structures: fabrication and characterization

1 Introduction

The formation of non-equilibrium morphological systems, which mimic the spontaneous pattern formation in nature, has been under extensive investigation [2,3]. It has been shown since the pioneering work of Mullins and Sekerka [4] that a growing spherical nucleus becomes unstable as its radius exceeds few times a critical one. Such an instability may usually leads to a dendritic growth giving rise to non-equilibrium morphologies. However if the dynamics of dendrite structure growth has been extensively studied, the relaxation of their resulting non-equilibrium shape after the growth is less investigated. In fact, in complex systems the relaxation dynamics can be quite complicated, and the search for dynamics scaling and universality is recent [5].

Cluster deposition has opened new ways for growing nano-structures on surfaces with a large diversity of non-equilibrium shapes [6–8]. Among these objects the concept of fractal, which is now accepted to characterize various morphologies in nature, can be used to reflect the complex nature of the dynamical processes underlying their stability. We have recently shown that the fractal islands, obtained by silver cluster deposition, fragment into many pieces, without changing the fractal dimension, when impurity is added to the incoming clusters [1] as expected from an increase of the surface self-diffusion of the silver atoms along the fractal arms. In the search of universality, it is then of fundamental interest to follow the shape change of fractal island when the atomic mobility is increased by thermal effect. A previous experiment has shown that fractal islands of gold grown at room temperature on Ru terraces removed their fractal shape to the benefit of a compact one upon annealing to 650 K [9]. However more recent numerical simulations involving atomic surface self-diffusion mechanism show that under thermal annealing of a fractal aggregate, its branch width first increases followed by the fractal fragmentation [10,11].

Here we report on experimental investigations of the thermal relaxation of nano-fractal antimony islands. The initial pattern is prepared by deposition of preformed antimony clusters on graphite surface, and the fractal dimension of the resulting islands is determined by the mass-radius relation. We show evidence that thermal annealing increases the width of the fractal arms, and that the time dependence of the arm-width evolves as predicted by a surface self-diffusion of the atoms along the arms. Furthermore we demonstrate that as time increases the fractal finally breaks into pieces. Comparison is done with silver fractal island fragmentation when impurity is added to the incident clusters, since in this last case fractal breaks into pieces without a substantial arm width broadening.

2 Experiment

Gas phase neutral antimony clusters are produced by a gas-aggregation type source [8]. Antimony vapor created in an 800 K crucible effuses into a mixture of He gas (17 mbar pressure) and Ar/N_2 gas (3 mbar pressure). Downstream from the oven, the nucleation takes place in a copper tube cooled with flowing liquid nitrogen.

[a] e-mail: catherine.brechignac@lac.u-psud.fr

The neutral cluster distribution enters a multiplate ionizing acceleration region, where it is ionized using a laser pulse, accelerated, and analyzed in size and composition with a time-of-flight mass spectrometer. As previously shown in gas phase cluster experiments, at low laser fluence, the resulting ion distribution does not depend on the laser flux and reflects the neutral distribution. It shows a Gaussian-like shape that allows us to determine the mean size of the clusters. The maximum of the cluster distribution $\langle n \rangle$ and its width depend on the cluster source conditions (temperature, pressure...). The full-width at half-maximum of the distribution of the cluster diameter is typically 20−25% of the mean value.

After deactivating the accelerating voltage of the time of flight, the neutral cluster distribution is deposited at low impact energy (0.05 eV/atom) and at room temperature, onto a cleaved graphite surface (HOPG). The bare substrates were previously heated at 700 °C during several hours and maintained in high vacuum (10^{-9} torr). A crystal quartz microbalance is inserted at right angles to the cluster beam and measures the flux of the incident neutral clusters. Removing the crystal quartz microbalance, the surface of graphite, is introduced perpendicular to the beam. The deposition time, from 1 to 20 minutes, is chosen depending on the cluster beam flux and the desired coverage. In our experiments, fluxes of the order of 10^{10} clusters/cm^2 s were used. Since per-atom kinetic energy of the incident clusters is very low compared with the binding energy of the metal clusters (1 to 3 eV), fragmentation of the incident cluster is unlikely and the clusters migrate on the surface as a whole and grow into fractal islands, when their size exceeds 150 atoms per cluster [8].

The prepared samples were transferred into a high vacuum chamber, where they are heated during a time duration t, varying from 10 minutes to few tens of hours. In our experiment two heating temperatures were chosen: $T = 180$ °C and $T = 200$ °C. After heating, the samples are cooled to room temperature before being imaged either in high vacuum with a non-contact Atomic Force Microscope (AFM) or after transfer in air with a scanning transmission electron microscope (STEM) operating at 100 kV and equipped with a field emission gun. The similarity between the images of the same sample obtained from the two microscopes (Figs. 1a and 1d) shows that the transfer in air does not affect the island morphologies. Moreover, we verified by imaging successively the same sample that the island pattern after air exposure does not evolve over periods of weeks, presumably because it is hindered by a buffer layer, which prevents the surface self-diffusion on the islands. For a given deposition, two samples were prepared and only one is heated at T during the time t, in order to get rid of the graphite substrate effect. Then the fractal branch width of the heated sample is referred to the unheated one.

3 Results and discussion

Figure 1 shows typical STEM images (left column) and non-contact AFM images (right column) of films of deposited 500-atom antimony clusters (1.5ML). Top images 1a and 1d have been obtained by STEM and AFM respectively, directly after the cluster deposition, without heating the samples. They show fractal islands, with a fractal dimension of 1.7 ± 0.1, deduced by using the power law relation between the mass and the gyration radius. In Figure 1d the width of the branches is mainly due to the dimension of the tip. Images 1b, 1c, and 1e were obtained after heating the samples at the end of the cluster depositions. Figures 1c and 1d images correspond to samples annealed at $T = 180$ °C during 160 mn and 870 mn respectively, before imaging. Image 1e correspond to a sample heated at $T = 200$ °C during 30 mn before imaging. Image 1f shows a measure of the height of the branch imaged by AFM. We have shown that the distribution and population of islands remain unaffected by heating, but clear changes in their morphology are apparent upon thermal annealing. For both temperatures the branch-width increases as time increases. Moreover the branch increases faster at higher temperature. It has to be noted that in both cases fingers break into small pieces during annealing.

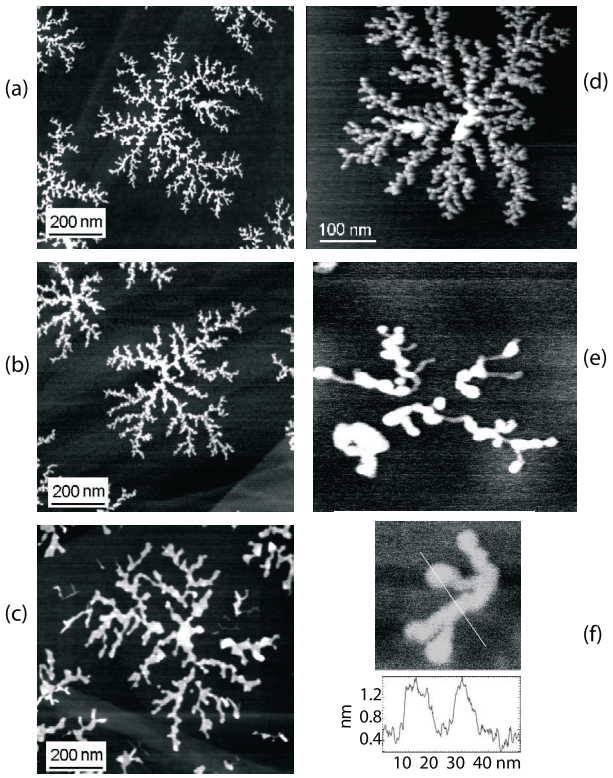

Fig. 1. Film of nano-fractal island obtained from deposition of 500-atom antimony clusters on graphite, as a function of heating time for two different temperatures (see the text). Left column (a, b, c): imaged from STEM, after heating at $T = 180$ °C, during 160 mn (b) and 870 mn (c); right column (d, e): imaged with non-contact AFM sample after heating at $T = 200$ °C during 30 mn. In AFM image the branch width is influenced by the tip broadening. Nevertheless, a broadening of the branch width is clearly observed as well as fractal fragmentation at longer time.

In thermal shape relaxation three main mass transport mechanisms may be involved.

(i) Evaporation-condensation mechanism, also called Oswald ripening mechanism, where atoms leave the island and move onto the substrate to recondensate somewhere else, (ii) surface self-diffusion process where only surface atoms migrate along island surface leading to smoother structure, (iii) viscous flow for which volume atoms are also mobile. The temporal evolution of the shape reflects the relaxation mechanism. Since the temporal evolution of the shape is driven by local deformation, one can write for a fractal shape $l \propto t^{\gamma}$, where l is the arm width of the fractal island, with γ depending on the relaxation mechanism. Numerical methods were used to model two kinds of sintering mechanisms in 2-dimensional systems, by surface self-diffusion, or by viscous flow [11]. The exponent γ, deduced from scaling argument is $\gamma = 1/4$ for the surface diffusion, and $\gamma = 1$ for viscous flow [11]. From macroscopic phenomenological argument [12], Irisawa *et al.* [10] evaluate $\gamma = 1/4$ for surface diffusion, and $\gamma = 1/2$ for Oswald ripening mechanism. However, the temporal shape relaxation depends also on the temperature: the shape relaxes faster at high temperature than at low one. Following the Arrhenius law one can assume that the time to move one atom varies as $t \propto \exp^{-E/kT}$, where E is the activation energy barrier involved in the mass transport, *i.e.* the energy that one atom has to surpass to move. It is well-known that E depends on the mass transport mechanism. It is smaller for surface diffusion than for Oswald ripening and viscous flow. Since the faster process controls the relaxation, one should obtain that at a given temperature, the shape relaxation is governed by surface self-diffusion at the beginning of the heating followed by viscous flow and,or Oswald ripening mechanism. Depending on the temperature, the time range where surface self-diffusion occurs can considerably vary. In our experiment the binding energy of a metal atom in the island is more than one order of magnitude larger than the adhesion energy of an antimony atom onto the graphite. So that the ejection of one atom from the island should imply to heat the substrate up to a temperature for which the atom will immediately evaporate from the substrate, making of coure unlikely the Oswald ripening mechanism. In order to avoid evaporation we restrict the heating temperature to low values.

Figure 2 shows the evolution of the ratio of the fractal arm-width l after heating at 180 °C to the unheated one l_0 as a function of time in logarithmic scale, together with the expected behaviors from surface diffusion (solid line) and viscous flow mass transport (dashed line). It is clearly seen that, at such a temperature and in the experimental time range, our measurements lie on the solid line indicating the surface self-diffusion as the dominant process for the fractal relaxation.

To go further we have performed Monte Carlo simulations, following the work of Irisawa *et al.* [10]. We started with a supported two-dimensional DLA fractal [13] with a given arm-width and use the waiting time algorithm [14]. The rate of adatoms to diffuse on the surface is set to unity. The rate of diffusion along the island periphery is $\exp[-mE_b/kT - nE_d/kT]$, where m is the number of bonds to be broken when atom moves and E_b is the bond energy. E_d is the barrier energy per bond and n is the number of neighboring bonds for an atom, which diffuses along the fractal island. The rate for evaporation of an atom from the island to become an adatom, which move randomly on the surface is given by $\exp[-rE_b/kT - \Delta\mu/kT]$, where r is the number of bonds that break when atom leaves the island and $\Delta\mu$ is the chemical potential involved in the growth process. Figure 3 shows the result of our simulation for $E_b/kT = 3$, $E_d/kT = 1$ and $\Delta\mu = 100$ both for morphology change and branch width as a function of time. Even if these parameters are chosen to be one order of magnitude smaller than in real experiment for having a reasonable computation time, their relative values are consistent with the experimental parameters. Moreover for

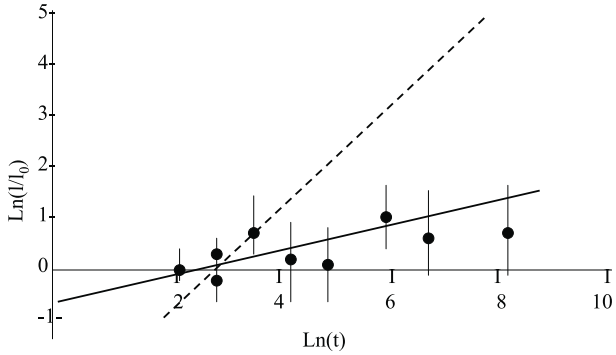

Fig. 2. Evolution of the ratio of the fractal branch-width l of Figure 1 heated at 180 °C and the unheated one l_0 as a function of time in logarithmic scale, together with the expected behaviors from surface self-diffusion relaxation process (solid line) and viscous flow mechanism (dashed line). The errors bars show the dispersion of the width along the arm.

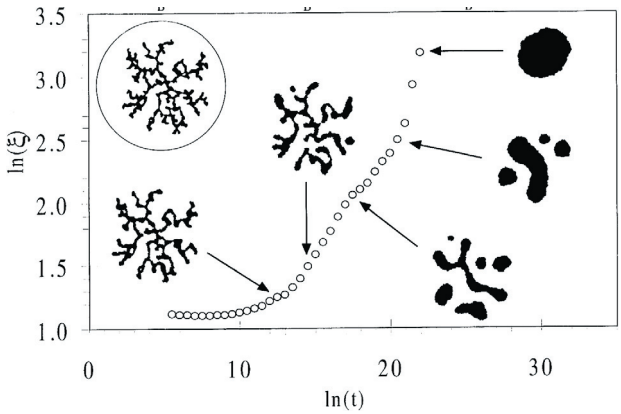

Fig. 3. Morphological change of a fractal island by thermal relaxation with the parameters $E_b/kT = 3$, $E_d/kT = 1$ and $\Delta\mu = 100$, together with the branch width of the fractal island as a function of time. In the first part of the curve the time is too short to observe any atomic motion: the branch width remains constant. At $\mathrm{Ln}(t) = 12$ the curve increases and follows the behavior expected for surface self-diffusion as time increases. For $\mathrm{Ln}(t)$ larger than 22 the branch-width follows the Oswald ripening behavior.

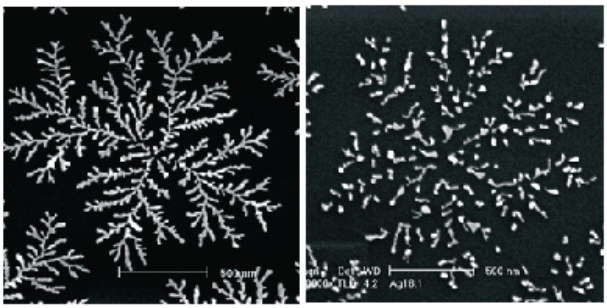

Fig. 4. STEM images of silver fractal islands. STEM images of silver fractal islands. Left image (a) is obtained from deposition of pure 150-atom clusters on graphite, right image (b) is obtained from deposition of 150-atom cluster carrying impurity. In this last case a spectacular fragmentation of the branches takes place.

sake of simplicity we have kept constant the number of atoms *i.e.* the Oswald ripening mechanism prevails over the evaporation in gas phase. It is clear that for a chosen temperature the relaxation process starts with surface self-diffusion which is the faster process at the beginning of the annealing and evolves to evaporation-condensation as time is going, in agreement with the ordering of the γ coefficients. Moreover the morphological evolution shows fragmentation events when surface self-diffusion governs the relaxation in agreement with the experimental results of Figure 1.

4 Comparison with chemically induced relaxation

From a previous experiment on silver cluster deposition on graphite, we have shown [2] that by adding trace amount of oxygen impurity in the incident silver clusters and keeping constant the temperature, a spectacular fragmentation of the fractal island takes place without noticeable arm broadening, as shown in Figure 4. An overall characterization of the deposited film shows evidence of a fragmentation induced by capillary instabilities through surface self-diffusion mechanism as predicted by Rayleigh for the break up of a cylindrical column [15]. It is then interesting to compare the experiments involving chemical and thermal relaxation, since both imply the surface self-diffusion mechanism.

In silver experiment, the number of fragments is directly connected to the Rayleigh's criterion for which a cylinder fragments when its length to its diameter ratio exceeds 4.5 [15]. Then for a cylinder with a ratio X between its length and its diameter, the number of fragments associated to surface diffusion relaxation should be in the order of $X/4.5$. Regarding the non-fragmented silver fractal of Figure 4a island as a set of bars with a set of length over diameter ratio X, the estimated number of fragments following the Rayleigh's criterion agrees with the experimental observation.

In antimony experiment, we consider the fractal islands having similar size than the ones in silver experiment. The observed number of fragments is smaller in antimony case than in silver one. Two reasons may be invoked to interpret the data. In silver experiment the role of the impurity is assumed to decrease E_d keeping E_b and the temperature T constant, whereas in antimony experiment, increasing the temperature decreases both E_d/kT and E_b/kT. This may influence the broadening of the arms during the annealing process and in turn the number of fragments. The second reason concerns the characteristic local length, since the evolution of the shape is driven by local deformations [5,10]. The comparison is done for the two non-fragmented fractal islands having similar global size and similar fractal dimension, and imaged in the same conditions by STEM. Looking at the Figure 1a for antimony, and Figure 4a for silver, differences in their shapes appear. In silver case the branches are more straight than in antimony case, and it is easier to define the X ratio. In antimony case, the branches are more tortuous, so that it is uneasy to apply the Rayleigh's criterion in the local length scale.

5 Conclusion

In conclusion, we have shown on the light of two examples of non equilibrium shape relaxation, *i.e.* thermal or chemical induced fractal relaxation, that fragmentation, which is an ubiquitous process, can be used to get insight into the mass transport mechanisms at nanoscale.

References

1. C. Bréchignac, Ph. Cahuzac, F. Carlier, C. Colliex, J. Le Roux, A. Masson, B. Yoon, U. Landman, Phys. Rev. Lett. **88**, 196103 (2002)
2. D'Arcy Thompson, *On Growth and Form* (Cambridge University Press, 1961)
3. J.S. Langer, Rev. Mod. Phys. **52**, 1 (1980)
4. W.W. Mullins, R.F. Sekerka, J. Appl. Phys. **34**, 323 (1963)
5. M. Conti, B. Meerson, P.V. Sasorov, Phys. Rev. Lett. **80**, 4693 (1998)
6. P. Jensen, Rev. Mod. Phys. **71**, 1695 (1999)
7. G.M. Francis, L. Kuipers, J.R.A. Cleaver, R.E. Palmer, J. Appl. Phys. **79**, 2942 (1996)
8. B. Yoon, V.M. Akulin, Ph. Cahuzac, F. Carlier, M. de Frutos, A. Masson, C. Mory, C. Colliex, C. Bréchignac, Surf. Sci. **443**, 76 (1999)
9. R.Q. Hwang, J. Schröder, C. Günther, R.J. Behm, Phys. Rev. Lett. **67**, 3279 (1991)
10. T. Irisawa, M. Uwaha, Y. Saito, Eur. Phys. Lett. **30**, 139 (1995)
11. N. Olivi-Tran, R. Thouy, R. Julien, J. Phys. France **6**, 557 (1996)
12. C. Herring, J. Appl. Phys. **21**, 301 (1950)
13. T.A. Witten, L.M. Sander, Phys. Rev. Lett. **47**, 1400 (1981)
14. G.H. Gilmer, J. Cryst. Growth **35**, 15 (1976)
15. J.W.S. Rayleigh, Proc. Lond. Math. Soc. **10**, 4 (1879)